

# Refining Airway Segmentation Through Breakage Filling and Leakage Reduction Using Point Clouds

Yan Hu, Erik Meijering, Yang Song

**Abstract**—Bronchoscopy reveals air passages and internal tissues for accurate diagnosis of various lung diseases. Robot-assisted bronchoscopy using an airway tree model can help path planning before surgery and navigation during surgery. In airway tree modeling, though volumetric deep learning methods have achieved good performance for airway segmentation, it remains a challenge due to the breakages and leakages. Some existing methods adopt post-processing using traditional methods like morphological and fuzzy connected algorithms. Also, some methods convert the volumetric data to point cloud format to refine segmentation. In this paper, we develop a new point cloud-based approach to refine volumetric segmentation. To address the breakage issue, we approach it as a regression problem of the branch extension direction and length. To tackle the leakage issue, we approach it as a segmentation task to eliminate leakages caused by breakage filling and from volumetric segmentation. Moreover, the direction information of branches is crucial for constructing the airway tree while point clouds do not naturally encode it. To introduce this information, we propose a directional feature aggregation, which first decomposes features of neighboring points based on their locations and aggregates decomposed features to aid the network in capturing the directional information effectively. Our proposed model has been evaluated on two public datasets, and the results show that our refinement can improve the volumetric segmentation.

## I. INTRODUCTION

Bronchoscopy is a diagnostic and therapeutic approach that allows doctors to view air passages and internal tissues to diagnose and make treatment plans for bronchial cancer, airway obstruction, and so on. Bronchoscopy examination is invasive and painful depending on the expert knowledge of physicians to plan bronchoscope trajectory [1]. However, a robot-assisted navigation bronchoscopy system can precisely target lesions or areas of interest, minimizing damage to surrounding healthy tissue and reducing the risk of procedural complications such as bleeding, or airway perforation. Fig. 1 shows the robot-assisted bronchoscopy system using the airway tree segmented from computed tomography (CT) to navigate the bronchoscope in the examination. Airway segmentation can provide a detailed 3D visualization of the patient’s airway anatomy and be used to create a virtual bronchoscopic image [2], [3] integrated with augmented reality in a more advanced system to help precise localization and plan the trajectory of the bronchoscope.

Existing deep learning-based volumetric airway segmentation methods can accurately segment thick branches, while

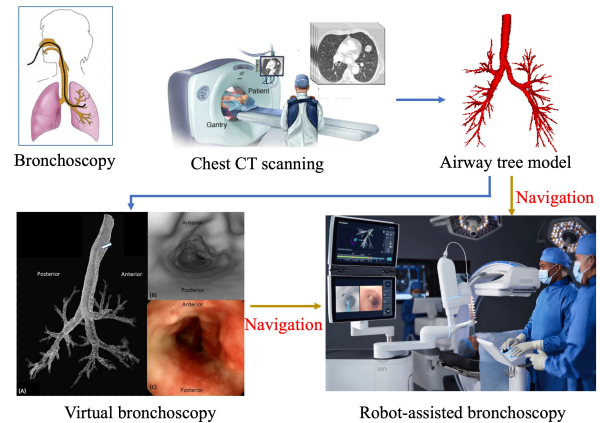


Fig. 1: An illustration of the robot-assisted bronchoscopy system, using segmentation of the airway tree to identify the best pathways for navigation<sup>1</sup>, and more advanced to simulate the actual bronchoscopy [6] pathway to plan the trajectory of the bronchoscope.

segmentation of thin branches remains challenging because of false negatives (breakages) and false positives (leakages including connective and extraneous segments), as shown in Fig. 3. Leakages can lead to the bronchoscope being navigated towards non-existent or incorrect paths, potentially causing harm to the patient. Breakages prevent the bronchoscope from accessing certain areas of airway, or increase the risk of accidental injury by forcing the procedure through uncharted or tighter passages. Therefore, enhancing the accuracy of airway segmentation via breakage filling and leakage reduction can provide more precise navigation during bronchoscopy examinations.

Theoretically, breakages and leakages can be attributed to the lack of global context and long-range dependencies because volumetric segmentation methods crop patches from the original CT volume. Early airway segmentation methods adopted traditional algorithms such as fuzzy connections [4], [5], to fill breakages and eliminate extraneous segments. However, these methods require a long time to process and are sensitive to hyper-parameters. Therefore, in this paper, we propose a fast and robust post-processing algorithm based on point clouds to refine airway segmentation.

Compared to volumetric segmentation, point clouds can

Yan Hu, Erik Meijering and Yang Song are with School of Computer Science and Engineering, University of New South Wales, Sydney, Australia {yan.hu2, erik.meijering, yang.song1}@unsw.edu.au.

<sup>1</sup>“UK first robotic-assisted lung biopsy procedures performed”, The Clinical Service Journal, <https://www.clinicalservicesjournal.com/story/42399/uk-first-robotic-assisted-lung-biopsy-procedures-performed>

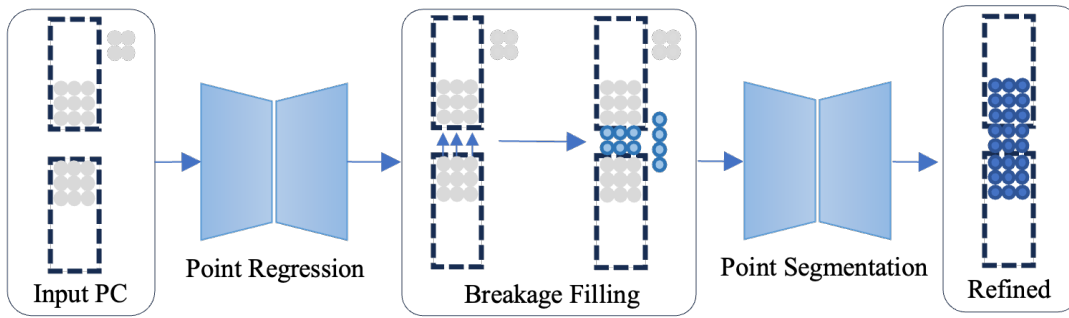


Fig. 2: Framework of the proposed segmentation refinement using point clouds. Gray points represent points sampled from the volumetric segmentation. Light blue points are generated by the breakage filling processing, and dark blue points are identified as points on the airway tree through the point segmentation network (leakage reduction).

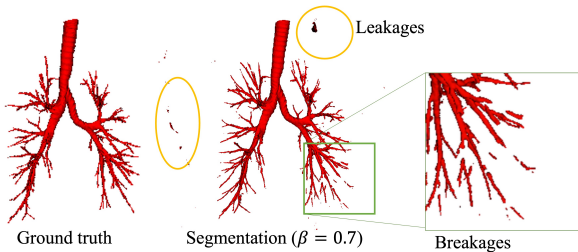


Fig. 3: Example of breakages and leakages.

leverage the sparse representation of large objects with far fewer computing resources. Some previous studies [7], [8], [9], [10], [11], [12] have proposed to refine or analyze the large and sparse objects using point clouds classification and segmentation. For example, Balsiger et al. [7] proposed to refine the tubular nerve segmentation via a point-wise classification task to reduce leakages. Yang et al. [8] sampled point clouds on the mesh of aneurysms and then used point clouds to perform fine-grained classification and segmentation. These studies adopted classical networks, such as PointNet [13], PointNet++ [14], KPConv [15], PointCNN [16], proving that point clouds classification/segmentation can effectively remove false positives because point clouds provide more comprehensive structures. However, classical point cloud networks lack the specialized mechanisms to effectively process and interpret thin, continuous, and complex tubular shapes, resulting in secondary breakages. We also note that explicit analysis of spatial orientation or direction of branches can help the model more reliably distinguish between the airway tree and leakages. Therefore, we propose a directional feature aggregation to model the direction of branches in the network design.

Moreover, since breakage filling requires extra points to be generated, it remains a problem if only using simple point clouds segmentation. Theoretically, point completion can help mitigate the breakage problem. However, it struggles with maintaining structural information and fine-grained reconstruction due to the appearance of artifacts and unrealistic distortion [17], and hence cannot be effectively applied to airway refinement due to the complex tubular shape. To

preserve the fine-grained tubular structures originally present and generate new points, we address the breakage filling via regressing the direction and length airway branches extend.

Overall, in this paper, we propose a point clouds-based refinement method to address breakages and leakages that occur in volumetric segmentation of airways in CT images. A regression network is first designed to predict the branch extension direction and length for generating new points to fill breakages without affecting the fine-grained shape of original point clouds. Then a segmentation network is adopted to remove leakages. Moreover, we propose a directional feature aggregation technique to better capture the branch directional representation in the networks of regression and segmentation because the branch direction aids in maintaining the connectivity of segments. We evaluated our proposed post-processing approach on two public datasets, and our method achieved a large performance gain compared to the volumetric segmentation. Our experiments also show that volumetric segmentation of high recall combined with a point clouds-based refinement can produce better airway segmentation.

In summary, our contributions are as follows:

- We propose a point cloud-based framework to refine volumetric airway segmentation results, in which breakages are first filled by regressing the direction and length of branch extension, and leakages are then removed through point clouds segmentation.
- We propose a directional feature aggregation to better learn branch directional information for mitigating secondary breakages caused by breakage filling and improving leakage reduction accuracy.
- We propose a breakage-filling strategy to generate new points on breakages based on the regressed branch extension direction and length.

## II. METHOD

### A. Overview

Fig. 2 shows the framework of using point clouds to refine the airway segmentation. The input point cloud consists of all points identified as airways by the volumetric segmentation result. We first build a regression network to predict the

direction and length of branch extension, and breakages are filled based on the regression output. Then, we build a segmentation network to identify whether input points are on the airway tree to reduce leakages. The details of breakage filling and leakage reduction are described in Section II-B and Section II-C, respectively. Moreover, in Section II-D, we propose a directional feature aggregation and build regression and segmentation networks by inserting it into PointNet++ to better capture the branch direction representations. Implementation details are provided in Section II-E

### B. Breakage Filling

Applying post-processing techniques to enhance the connectivity for linking segments can address breakages in volumetric segmentation. The connectivity by the branch direction and extension length provides the spatial orientation and scale of the branch to estimate the missing parts. Therefore, we formulate the breakage filling as a regression task of the branch direction and extension length. It consists of two components: (1) **building the direction vector** of each airway voxel as the ground truth in the training phase, and (2) **filling breakages** with the predicted direction vector and the branch length in the testing phase.

1) *Building the Direction Vector*: Fig. 4 (a) demonstrates the direction vector definition from the projection on the  $x-z$  plane. Given a tubular airway tree, we define the direction from the root to the branch as the positive direction. First, we extract the skeleton and convert it into a point set  $P$ , and define a series of query spheres  $\{B_{r_0}, B_{r_1}, \dots, B_{r_N}\}$  with increasing radius. For any given point  $p$  from  $P$ , there are two crosspoints  $c_{r_0}$  and  $c'_{r_0}$  (as shown in Fig. 4 (a)) between the skeleton and the smallest query sphere  $B_{r_0}$  forming two vectors  $\overrightarrow{p, c_{r_0}}$  (positive direction) and  $\overrightarrow{p, c'_{r_0}}$  (negative direction), however, only  $\overrightarrow{p, c_{r_0}}$  is used.  $\overrightarrow{p, c_{r_0}} = (d_x, d_y, d_z)$  is the direction vector from  $p$  to  $c_{r_0}$ , representing initial tubular branch extension. Similarly, we can obtain the other direction vectors  $\{\overrightarrow{p, c_{r_1}}, \dots, \overrightarrow{p, c_{r_N}}\}$  from the query spheres  $\{B_{r_1}, \dots, B_{r_N}\}$ . Then,  $\overrightarrow{p, c_{r_0}}$  is set as the initial direction vector, and we compute deviating angles to  $\{\overrightarrow{p, c_{r_1}}, \dots, \overrightarrow{p, c_{r_N}}\}$ , denoted as  $\{\theta_1, \dots, \theta_N\}$ . If the deviating angle  $\theta_i$  is smaller than the threshold  $\theta_T$ , we assume that the direction vector  $\overrightarrow{p, c_{r_i}}$  extends following the initial direction vector and the extension length is  $r_i$ . Finally, we concatenate the initial direction vector coordinate and maximum extension length as direction vector  $[d_x, d_y, d_z, r]$  for  $p$ .

We assume that points on the same branch with the same  $z$ -axis coordinate have the same direction vector. As illustrated in Fig. 4 (a), the light arrows are copied from the corresponding dark arrows. Note that crosspoints obtained on different branches are ignored to compute the deviating angle. The radius of query spheres is set as  $\{2, 3, 4, 5, 6\}$  voxels to compute the deviating angles since breakages on the thin branch are usually in a small length, and the threshold of deviating angle  $\theta_T$  is set as  $20^\circ$  because a too large threshold increases the length estimation error.

2) *Filling Breakages*: For a given point  $p$ , the regression network predicts the initial direction vector coordinate

$[\hat{d}_x, \hat{d}_y, \hat{d}_z]$  and maximum extension length  $\hat{r}$ . According to the approximation of extension length, all points located on the direction of the initial direction vector and satisfying the distance to point  $p$  less than  $\hat{r}$  should be considered as the airway tree.

PointNet++ for segmentation [14] is adopted as the backbone to build the regression network, but the original prediction header is replaced by two separate headers, i.e., the initial vector direction regression header and extension length regression header, with three dense layers, respectively. Directional feature aggregation (Section II-D) is inserted into the regression headers before each dense layer to enhance the initial direction vector and extension length learning.

### C. Leakage Reduction

Since the process of filling breakages may introduce extra false positives (light blue points outside of the tube in Fig. 2), the input for leakage reduction consists of a combination of volumetric segmentation and the output of breakage filling and is formulated as a point clouds segmentation task. PointNet++ [14] is adopted as the backbone to build the leakage reduction, but the final layer is modified as a two-class output (true positive airway points and false positive leakage points). Similarly, directional feature aggregation (Section II-D) is inserted into the input layer of the prediction header.

### D. Directional Feature Aggregation

The direction of branches is an important geometric description for airway segmentation. However, point clouds are essentially unstructured data and do not encode directional information, so no inherent information about the connectivity to other points for each independent point is provided. Aggregating features from neighborhoods can introduce connectivity of points, but the direction is still lacking via direct merging. To extract directional information from point clouds, we propose a directional feature aggregation, which projects features of neighborhoods based on the relative location between center point and its neighborhoods to perform direction-specific processing in aggregation.

For a given point  $p$  and a search ball with radius  $r$ , neighboring points within the search ball are represented by  $Q = \{q_1, q_2, \dots, q_N\}$ . Taking the feature projection from  $q_1$  to  $p$  as an example, the projection vectors of  $\overrightarrow{q_1, p}$  are  $\{w_x, w_y, w_z\}$ , and three corresponding intersection angles  $\{\theta_{w_x}, \theta_{w_y}, \theta_{w_z}\}$ . The projected features of  $q_i$  to  $p$  are then computed as:

$$F'_{\overrightarrow{q_1, p}} = ((F_{q_i} \cos(\theta_{w_x}), F_{q_i} \cos(\theta_{w_y}), F_{q_i} \cos(\theta_{w_z})) \quad (1)$$

The aggregated feature from neighborhoods of  $p$  with directional decomposition is:

$$F'_p = [Conv(\sum_{q_i \in Q} F_{q_i} \cos(\theta_{w_x})), Conv(\sum_{q_i \in Q} F_{q_i} \cos(\theta_{w_y})), Conv(\sum_{q_i \in Q} F_{q_i} \cos(\theta_{w_z}))] \quad (2)$$

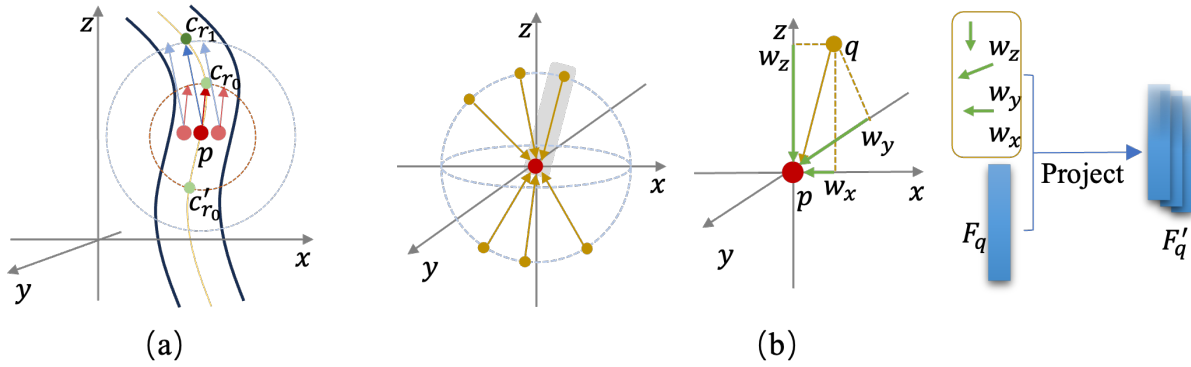


Fig. 4: Illustration of direction vector definition by 2D projection on  $x-z$  plane (a) and directional feature aggregation (b). In (a), for a given point  $p$  (red point) on the skeleton (yellow line) and two predefined search spheres,  $\overrightarrow{p, c_{r_0}}$  is the initial direction vector (dark red arrow). For the crosspoint  $c_{r_1}$ , the deviating angle is defined as the angle between  $\overrightarrow{p, c_{r_0}}$  and  $\overrightarrow{p, c_{r_1}}$  (dark blue arrow). In (b), features are projected in three directions to get decomposed features of  $q_i$  to  $q$ .

where  $[\cdot]$  represents concatenation and  $Conv(\cdot)$  denotes the convolution layer with kernel size of 1.

### E. Implementation

1) *Loss Function*: A weighted cross-entropy loss is used for the point clouds segmentation task, where points on the skeleton have a weight of 10 and others a weight of 1. Mean square error loss is used for the initial vector regression and the extension length regression.

2) *Training Details*: We adopted UNet3D as the baseline volumetric segmentation model (initial channel of 32, input size of  $96 \times 96 \times 96$ , and deep supervision from the decoder with sizes of  $48 \times 48 \times 48$  and  $24 \times 24 \times 24$ , using Tversky loss [18]). We extract the feature vector of each point from the volumetric probability ( $5 \times 5 \times 5$  neighborhood) as the point feature to feed into two point clouds networks with 8096 points. Python library<sup>2</sup> is adopted to extract the skeleton from volumetric segmentation.

Adam is adopted as the optimizer, with learning rates of  $10^{-4}$  and  $10^{-5}$ , number of epochs of 50 and 80, and batch size of 8 for regression and segmentation networks, respectively. Experiments are performed on 1 NVIDIA RTX 3090 with 24GB memory using TensorFlow 2.4.0.

## III. EXPERIMENT

### A. Datasets

We evaluated our proposed refinement method on two public datasets. (1) the Binary Airway Segmentation Dataset (BAS) of 90 cases, in which 20 cases are from the EXACT'09 Challenge [19] training set and 70 cases are from the Lung Image Database Consortium image collection (LIDC-IDRI). It is split into the training (50 cases), validation (20 cases), and testing (20 cases) sets following [20]. (2) Multi-site, Multi-Domain Airway Tree Modeling (ATM'22) Challenge Dataset, which consists of 300 training cases and 50 validation cases. The evaluation on the ATM'22 dataset was done by the online validation system.

<sup>2</sup>[https://github.com/scikit-image/scikit-image/blob/main/skimage/morphology/\\_skeletonize.py](https://github.com/scikit-image/scikit-image/blob/main/skimage/morphology/_skeletonize.py)

### B. Evaluation Metrics

To evaluate our model and make a fair comparison with other methods, we followed four widely used metrics from other studies [21]: (1) precision, (2) the Dice similarity coefficient (Dice), (3) the ratio of tree length detected (TD), and (4) the ratio of branches detected (BD). According to the definition of the metrics, higher Dice and precision mean fewer breakages, and higher TD means fewer breakages in the segmentation.

### C. Results Comparison

Table I shows the results of UNet3D trained by Tversky loss with multiple  $\beta$  settings. According to the definition of Tversky loss [18],  $\beta$  is used to trade off precision and recall. In the comparison of UNet3D results, both TD and BD show obvious improvements while Dice decreases as  $\beta$  increases from 0.3 to 0.7 because the increase in  $\beta$  is biased toward recall, resulting in more false positives. However, TD and BD decrease when  $\beta$  rises from 0.7 to 0.9 while Dice and precision increase. The trade-off between accuracy and recall is hard to balance in the volumetric airway segmentation. UNet3D trained using  $\beta = 0.7$  achieves the best results, so it is adopted as the baseline of volumetric segmentation to perform refinement using point clouds, marked as UNet3D\*. Compared to pure UNet3D, our point clouds-based refinement brings a large performance gain in Dice and precision and also improves the TD and BD.

We also compare our proposed methods to three top airway segmentation methods, which include specific improvements to address the breakage and leakage issues. Specifically, Qin et al. [22] adopted feature recalibration and attention distillation, Hu et al. [23] combined different topology-based loss functions, and Zheng et al. [20] proposed an optimization algorithm. Results of Qin et al. and Hu et al. are quoted from [23], and of Zheng et al. are quoted from [20]. These compared methods outperform our baseline UNet3D\* in most evaluation metrics. By incorporating our refinement method, the performance improves substantially

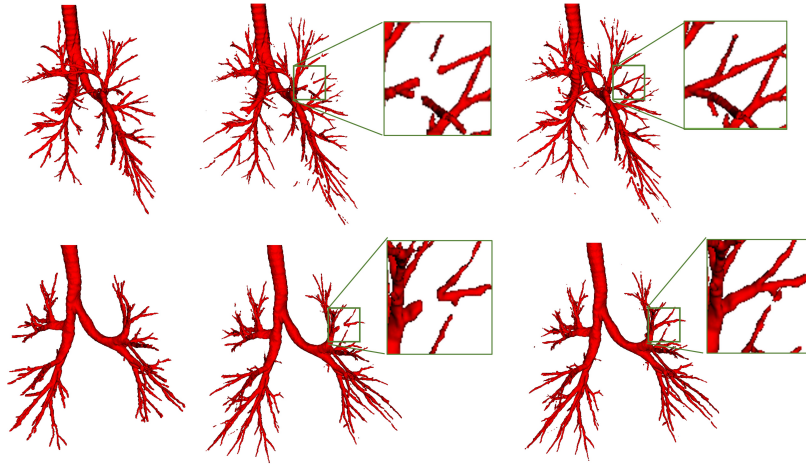


Fig. 5: Visual comparison. From left to right: ground truth, volumetric segmentation, and refined segmentation.

TABLE I: Comparison with other airway segmentation methods on the BAS dataset (first eight rows) and ATM’22 challenge validation dataset (last two rows).

Datasets	Methods	TD	BD	Dice	Precision
BAS	Qin et al. [22]	90.80	86.50	91.40	89.20
	Zheng et al. [20]	92.50	88.70	-	91.40
	Hu et al. [23]	93.10	89.40	<b>92.00</b>	92.30
	UNet3D ( $\beta = 0.3$ )	88.04	78.62	91.78	91.28
	UNet3D ( $\beta = 0.5$ )	91.68	84.98	91.74	90.87
	UNet3D* ( $\beta = 0.7$ )	93.73	88.92	89.85	86.22
	UNet3D ( $\beta = 0.9$ )	90.19	82.88	90.32	87.47
	Ours (UNet3D* + Refine)	<b>94.51</b>	<b>90.31</b>	91.72	<b>92.48</b>
ATM	UNet3D* ( $\beta = 0.7$ )	88.94	83.50	94.97	96.10
	Ours (UNet3D* + Refine)	<b>90.74</b>	<b>85.88</b>	94.91	<b>96.23</b>

TABLE II: Ablation studies of framework components and directional feature aggregation on the BAS dataset.

Methods	TD	BD	Dice	Precision
UNet3D*	93.73	88.92	89.85	86.22
UNet3D* + LR (w/o FeatDe)	91.31	86.57	90.69	88.04
UNet3D* + LR	93.20	87.84	90.60	87.99
UNet3D* + BF (w/o FeatDe)	94.33	90.37	72.92	61.36
UNet3D* + BF	<b>95.14</b>	<b>91.26</b>	80.99	76.96
UNet3D* + BF + LR (w/o FeatDe)	93.36	88.02	91.51	88.87
UNet3D* + BF + LR (Ours)	94.51	90.31	<b>91.72</b>	<b>92.48</b>

and exceeds the compared methods except for Dice, which leaves with a small gap (0.28%).

Furthermore, we report the results of the ATM’22 challenge validation dataset evaluated by the online system. Since the volumetric segmentation model we adopted is relatively simple compared to other methods reported in the benchmark [21], its performance on the leaderboard is not very high. However, our refinement method still resulted in a performance improvement compared to volumetric segmentation.

Fig. 5 shows the visual comparison of volumetric segmentation and refined results using point clouds. Compared with the ground truth, there are still leakages at the end of the thin branch that have not been removed. The possible reason is that the structural description of the airway tree learned by the leakage reduction network is not enough, and there are

also errors in the annotation of the ground truth. Compared to volumetric segmentation, the refined segmentation (see the zoom-in visualization) can narrow the breakages and connect segments when breakages are small. This is because when we define the directional vector, we set the length of the extension to be a maximum of 6 voxels. Therefore, if the breakage is too large, it cannot be completely filled.

#### D. Ablation Studies

To explore the effectiveness of our post-processing framework components and the directional feature aggregation, we perform corresponding ablation studies.

1) *Framework Components*: From Table II, it can be seen that the regression-based breakage filling increases the performance on TD and BD but causes Dice to decrease because extra points are generated. It may be attributed to

our definition of the direction vector on the same branch. However, when the search sphere of large diameter covers other branches, multiple intersection points can be obtained, which is ignored in the implementation. We also assume that the direction vector of the skeleton points equals the neighbor points. Such an assumption and approximation result in errors when building the ground truth.

Meanwhile, the results show leakage reduction refinement brings performance gain on Dice of UNet3D\*, proving that it can effectively remove breakages because point clouds bring more global structural information from the larger scope of the airway tree. However, although there is an improvement on Dice, the segmentation errors can disrupt the continuity of the airway, leading to a decrease in TD and BD.

In summary, the approach of filling breakages first and then removing leakages can achieve better results compared to the volumetric segmentation.

2) *Directional Feature Aggregation*: We remove all directional feature aggregation in the networks and report ablation results in Table II. In the context of breakage filling, incorporating directional feature aggregation enhances TD and BD, yet it compromises accuracy with a drop in Dice and precision, as it generates fewer false positives. For leakage reduction, the usage of directional feature aggregation contributes to producing fewer secondary breakages and a smaller decrease in TD and BD, while Dice and precision improve due to the effective removal of leakages. The combination of refinement results shows directional feature aggregation can bring an overall performance gain on the airway tree segmentation.

#### IV. CONCLUSION

In this paper, we proposed a point clouds-based airway segmentation refinement framework to improve the accuracy of building an airway tree model for robot-assisted bronchoscopy navigation. We formulate the breakage filling as a regression of branch extension direction and length and generate points on branch extensions to fill breakages. And the leakage reduction is formulated as a point clouds segmentation task. Moreover, a directional feature aggregation operation is proposed to better capture the directional information of branches. Ablation studies of framework components show that, although breakage filling and leakage reduction have drawbacks, the combination of high recall volumetric segmentation and point clouds yields better performance.

#### REFERENCES

- [1] P. J. Reynisson, H. O. Leira, T. N. Hernes, E. F. Hofstad, M. Scali, H. Sorger, T. Amundsen, F. Lindseth, and T. Langø, "Navigated bronchoscopy: a technical review," *Journal of Bronchology & Interventional Pulmonology*, vol. 21, no. 3, pp. 242–264, 2014.
- [2] S. V. Kemp, "Navigation bronchoscopy," *Respiration*, vol. 99, no. 4, pp. 277–286, 2020.
- [3] M. Davoudi and H. G. Colt, "Bronchoscopy simulation: a brief review," *Advances in Health Sciences Education*, vol. 14, pp. 287–296, 2009.
- [4] F. Y. Rizi, A. Ahmadian, N. Rezaie, and S. A. Iranmanesh, "Leakage suppression in human airway tree segmentation using shape optimization based on fuzzy connectivity method," *International Journal of Imaging Systems and Technology*, vol. 23, no. 1, pp. 71–84, 2013.

- [5] J. K. Udupa and P. K. Saha, "Fuzzy connectedness and image segmentation," *Proceedings of the IEEE*, vol. 91, no. 10, pp. 1649–1669, 2003.
- [6] Y.-C. Chien, H.-C. Wang, Y.-C. Chang, and Y.-F. Chen, "Uncommon chronic cough caused by tracheobronchopathia osteochondroplastica," *Thorax*, vol. 67, no. 11, pp. 1021–1022, 2012.
- [7] F. Balsiger, Y. Soom, O. Scheidegger, and M. Reyes, "Learning shape representation on sparse point clouds for volumetric image segmentation," in *Medical Image Computing and Computer Assisted Intervention—MICCAI 2019: 22nd International Conference, Shenzhen, China, October 13–17, 2019, Proceedings, Part II 22*, pp. 273–281, Springer, 2019.
- [8] X. Yang, D. Xia, T. Kin, and T. Igarashi, "Intra: 3D intracranial aneurysm dataset for deep learning," in *Proceedings of the IEEE/CVF Conference on Computer Vision and Pattern Recognition*, pp. 2656–2666, 2020.
- [9] J. Yu, C. Zhang, H. Wang, D. Zhang, Y. Song, T. Xiang, D. Liu, and W. Cai, "3D medical point Transformer: Introducing convolution to attention networks for medical point cloud analysis," *arXiv preprint arXiv:2112.04863*, 2021.
- [10] T. Peng, Y. Wu, J. Qin, Q. J. Wu, and J. Cai, "H-ProSeg: Hybrid ultrasound prostate segmentation based on explainability-guided mathematical model," *Computer Methods and Programs in Biomedicine*, vol. 219, p. 106752, 2022.
- [11] P. Rygiel, M. Zieba, and T. Konopczynski, "Eigenvector grouping for point cloud vessel labeling," in *Geometric Deep Learning in Medical Image Analysis*, pp. 72–84, PMLR, 2022.
- [12] R. Zhao, H. Wang, C. Zhang, and W. Cai, "PointNeuron: 3D Neuron reconstruction via geometry and topology learning of point clouds," in *Proceedings of the IEEE/CVF Winter Conference on Applications of Computer Vision*, pp. 5787–5797, 2023.
- [13] C. R. Qi, H. Su, K. Mo, and L. J. Guibas, "PointNet: Deep learning on point sets for 3D classification and segmentation," in *Proceedings of the IEEE conference on Computer Vision and Pattern Recognition*, pp. 652–660, 2017.
- [14] C. R. Qi, L. Yi, H. Su, and L. J. Guibas, "PointNet++: Deep hierarchical feature learning on point sets in a metric space," *Advances in Neural Information Processing systems*, vol. 30, 2017.
- [15] H. Thomas, C. R. Qi, J.-E. Deschaud, B. Marcotegui, F. Goulette, and L. J. Guibas, "KPCConv: Flexible and deformable convolution for point clouds," in *Proceedings of the IEEE/CVF International Conference on Computer Vision*, pp. 6411–6420, 2019.
- [16] Y. Li, R. Bu, M. Sun, W. Wu, X. Di, and B. Chen, "PointCNN: Convolution on x-transformed points," *Advances in Neural Information Processing Systems*, vol. 31, 2018.
- [17] B. Fei, W. Yang, W.-M. Chen, Z. Li, Y. Li, T. Ma, X. Hu, and L. Ma, "Comprehensive review of deep learning-based 3d point cloud completion processing and analysis," *IEEE Transactions on Intelligent Transportation Systems*, vol. 23, no. 12, pp. 22862–22883, 2022.
- [18] S. S. M. Salehi, D. Erdogmus, and A. Gholipour, "Tversky loss function for image segmentation using 3D fully convolutional deep networks," in *International Workshop on Machine Learning in Medical Imaging*, pp. 379–387, Springer, 2017.
- [19] P. Lo, B. Van Ginneken, J. M. Reinhardt, T. Yavarna, P. A. De Jong, B. Irving, C. Fetita, M. Ortner, R. Pinho, J. Sijbers, et al., "Extraction of airways from CT (EXACT'09)," *IEEE Transactions on Medical Imaging*, vol. 31, no. 11, pp. 2093–2107, 2012.
- [20] H. Zheng, Y. Qin, Y. Gu, F. Xie, J. Yang, J. Sun, and G.-Z. Yang, "Alleviating class-wise gradient imbalance for pulmonary airway segmentation," *IEEE Transactions on Medical Imaging*, vol. 40, no. 9, pp. 2452–2462, 2021.
- [21] M. Zhang, Y. Wu, H. Zhang, Y. Qin, H. Zheng, W. Tang, C. Arnold, C. Pei, P. Yu, Y. Nan, et al., "Multi-site, multi-domain airway tree modeling," *Medical Image Analysis*, vol. 90, p. 102957, 2023.
- [22] Y. Qin, H. Zheng, Y. Gu, X. Huang, J. Yang, L. Wang, F. Yao, Y.-M. Zhu, and G.-Z. Yang, "Learning tubule-sensitive CNNs for pulmonary airway and artery-vein segmentation in CT," *IEEE Transactions on Medical Imaging*, vol. 40, no. 6, pp. 1603–1617, 2021.
- [23] Y. Hu, E. Meijering, and Y. Song, "Large-kernel attention network with distance regression and topological self-correction for airway segmentation," in *Australasian Joint Conference on Artificial Intelligence*, pp. 115–126, Springer, 2023.